



Original article

Cytotoxic effect of silver nanoparticles synthesized from ethanolic extract of *Allium sativum* on A549 lung cancer cell lineR. Padmini^a, V. Uma Maheshwari Nallal^a, M. Razia^{a,*}, S. Sivaramkrishnan^b, Hissah Abdulrahman Alodaini^c, Ashraf Atef Hatamleh^c, Munirah Abdullah Al-Dosary^c, Venkatalakshmi Ranganathan^{d,*}, Woo Jin Chung^e^a Department of Biotechnology, Mother Teresa Women's University, Kodaikanal 624101, Tamil Nadu, India^b Department of Biotechnology, Bharathidasan University, Palkalaiperur, Tiruchirappalli, Tamil Nadu, 620024, India^c Department of Botany and Microbiology, College of Science, King Saud University, P.O. Box 2455, Riyadh 11451, Saudi Arabia^d Faculty of pharmaceutical Sciences, UCSI University, 56000 Cheras, Kulala Lumpur, Malaysia^e Department of Environmental Energy and Engineering, Kyonggi University Yeongtong-Gu, Suwon, Gyeonggi-Do, 16227, Republic of Korea

ARTICLE INFO

Article history:

Received 8 December 2021

Revised 17 March 2022

Accepted 25 March 2022

Available online 30 March 2022

Keywords:

Green synthesis

Nanoparticles

Allium sativum

Cytotoxic activity

Human lung adenocarcinoma

A549 cells

ABSTRACT

Objectives: The present study was aimed to synthesize Silver nanoparticles (Ag NPs) from ethanol extract of *Allium sativum* to evaluate the *in-vitro* cytotoxicity effect on human lung adenocarcinoma cells (A549). **Methods:** Spectroscopic analysis were performed to determine the formation, stability, nature and the functional groups of the Ag NPs. Microscopic analysis were performed to ascertain the morphology and size of the particles. *In-vitro* MTT (3-(4,5-Dimethylthiazol-2-yl)-2,5-Diphenyltetrazolium Bromide) assay was performed to determine the cytotoxic potential of the Ag NPs on A549 lung cancer cell lines. **Results:** The UV-Visible spectrum confirmed the formation of the particles. Fourier Transform Infrared (FTIR) spectrum revealed the presence of carbonyl, carboxyl, primary and secondary amine groups. Powder X-ray diffraction (PXRD) established the crystalline nature and FCC structure of Ag NPs. Morphological analysis performed using Field Emission-Scanning Electron Microscopy (FESEM), High-Resolution Transmission Electron Microscopy (HRTEM), Selected Area Electron Diffraction (SAED) pattern showed spherical and rod shaped bio synthesized Ag NPs with variable size ranging from 20 nm to 40 nm. The synthesized Ag NPs showed a significant cytotoxic potential against A549 human lung cancer cells at an IC₅₀ of 22 µg/ml.

Conclusion: The present study revealed a cost-effective, simple and effective method to synthesize Ag NPs using garlic extract and the cytotoxic activity on human adenocarcinoma cells (A549) demonstrated their future application as potential anti-cancer agent.

© 2022 The Author(s). Published by Elsevier B.V. on behalf of King Saud University. This is an open access article under the CC BY-NC-ND license (<http://creativecommons.org/licenses/by-nc-nd/4.0/>).

1. Introduction

Nanotechnology is an interdisciplinary field in which tremendous number of materials were developed for various applications

* Corresponding authors.

E-mail addresses: razia.bt@motherteresawomenuniv.ac.in (M. Razia), rvenkatm-pharm@gmail.com, razia.bt@motherteresawomenuniv.ac.in, rvenkatm-pharm@gmail.com (V. Ranganathan).

Peer review under responsibility of King Saud University.



and found remarkable solutions in the field of medicine, biotechnology, energy conservation and water treatment. The Nanoparticles (NPs) are materials which has at least a dimension sized nanometers from 1 to 100 due to its larger surface area to volume ratio (Murugesan et al., 2017; Bouqellah et al., 2019; El-Refai et al., 2018). Metal NPs are gaining interest at present, due to their applications which include a drug delivery system, diagnostic assays and radiotherapy treatment (Selvan et al., 2010). Among the various metal NPs, Silver (Ag) and its oxides are of special interest owing to their exceptional physiochemical characteristics such as good conductivity, biochemical stability, catalytic activity (Pattanayak et al., 2017; Sevilla, 2013; Burda et al., 2005; Shume et al., 2020) and it is found that Ag NPs show minimal toxicological impacts compared to other noble metals (Susheela et al., 2013). It

has been reported that Ag NPs show promising cytotoxic activity against several cancer cell lines including MCF-7, A549, HeLa and HT29 cells. These findings suggest that Ag NPs play a remarkable role as an anticancer agent (Castro-Aceituno et al., 2016). Generally, Ag NPs colloidal solutions are obtained from Ag(I), using alcohols and amines as the reducing and/or the capping agents. But, most of the chemicals employed in these procedures are toxic to humans and the environment, and thus, a “green” synthesis method is required for the synthesis (Onitsuka et al., 2019). In this aspect, Senthilkumar et al., 2018 has developed plasmonic Ag NPs by green mediated synthesis using three variety of leaves extracts such as *Eucalyptus globus*, *Azadirachta indica* and *Coriandrum sativum*. Where, flavonoids and phenolic groups of the extracts are used for reducing AgNO₃ to metal ions compounds. Ocsy et al., 2017 has fabricated Ag NPs from green hydrothermal approach by using reducing agent of red cabbage extract. The prepared Ag NPs showed excellent inhibitory potential against gram positive and gram negative bacteria. The rapid green synthesis of Ag NPs has been developed from *Piper longum* catkin extract and reported by Jayapriya et al., 2019. The reduction of Ag NPs is achieved by exposed sunlight radiation. The phytoconstituents acts as the major role for reduction of AgNO₃ to Ag NPs. The prepared material has spherical in shape and size ranging from 15 to 40 nm. Philipa et al., 2011 has developed rapid green approach of spherical like Ag and Au NPs at ambient and heat (373 K) conditions from the reducing agent of *Murraya Koenigii* leaf extract. The percolated green approach of Ag NPs prepared via *C. Sativum* leaf, stem, root and seed extracts has superior antimicrobial activity against *Klebsiella pneumoniae* (Senthil et al., 2018). Several studies have also reported the successful synthesis of other nanoparticles using plant extracts such as *Aegle marmelos* leaf extract mediated Nickel oxide nanoparticles (Ezhilarasi et al., 2018), Zinc oxide nanoparticles using *Wattakaka volubilis* (Jeyabharathi et al., 2022) and Titanium dioxide nanoparticles using *Citrus sinensis* (Fall et al., 2020). Ag NPs synthesized using plant extracts are reported to demonstrate excellent antioxidant, antibacterial, antifungal and anti-cancer properties (Thomas et al., 2019; Valsalam et al., 2019). Hence, the recent reports proved that, plant extracts may act as better reducing and stabilizing agents and contribute a better platform for NPs synthesis as they are not harmful (He et al., 2016).

Garlic (*Allium sativum* L) contains an abundance of chemical compounds, which has been used for many decades, both as a flavoring and as folk herbal medicine. It also aids in the prevention of fatal disease such as cancer (Fleischauer and Arab, 2001). Garlic exhibits combined actions with other compounds that can inhibit proliferation of cancerous cells. Various studies have reported that garlic has an enhanced activity in cancer prevention owing to the sulphur containing biometabolites such as S-allyl cysteine, Diallyl sulfide and Allicin (Rahman and Billington, 2000). These bioactive compounds are involved in various mechanisms which include inhibition of incidence of cancer, inhibition of proliferation and free radical scavenging activities (Jin et al., 2013). In the recent decade, various metal NPs like Ag, Au and Pt have been used in carcinoma therapy against several types of cancer especially adenocarcinoma. Adenocarcinoma is a prevalent type of lung cancer which arises in the type II alveolar cells in smokers and non-smokers which includes men, women and children. Though it has a slow rate of progress the possibility of metastasis is high in this type of cancer (Zappa and Mousa, 2016). Hence, the present study focused to develop green synthesis of Ag NPs using ethanol extract of fresh garlic powder and also study about the anticancer activity using A549 lung cancer cell line.

2. Materials and methods

2.1. Materials for synthesis of Ag NPs

The plant was collected from Kodaikanal, Dindigul district of TamilNadu. The garlic bulbs were identified and authenticated by Prof. P. Jayaraman, Plant Anatomy Research Center, Tambaram, Chennai. The garlic bulbs were thoroughly cleaned and cut into small pieces, dried in open air atmosphere and crushed into fine powder. After that, obtained garlic powder was extracted using ethanol at boiling temperature for 48 h by Soxhlet extractor (Lin et al., 1999). Whatman No 1 filter paper was used to filter the extract and the solvent was removed using rotary vacuum evaporator and stored for further analysis.

2.2. Synthesis of Ag NPs via green approach

Initially, 1 mM of silver nitrate (AgNO₃) was added into 50 ml of double distilled (DD) water under constant stirring. After that, 5 ml of ethanol extract of fresh garlic powder was mixed with above mentioned solution. During the reaction process, the solution colour gradually changed light brown to dark brown at 3 hrs constant stirring which indicates the NPs formation. However, the polyphenols present in the garlic extracts act as reducing agent and cause the formation of Ag NPs. The formation of dark brown color (Fig. 1) demonstrates the synthesis of Ag₂O. The synthesized Ag₂O were centrifuged and the pellet was collected. The collected product was kept in a lyophilizer for 24 h, to obtain powdered form of a NPs. The obtained powder was stored at 4 °C for further characterization studies and cytotoxicity analysis (Selvan et al., 2018).

2.3. Characterization

The structure-based properties of Ag NPs was analyzed by powder X-ray diffraction (PXRD) pattern carried out by X' Pert instrument with Cu K α radiation. Molecular analysis of the Ag NPs was analysed by Fourier-Transform Infrared (Nicolet b6700) spectrometer using KBr pellet technique in the range from 4000 to 450 cm⁻¹. The characteristic absorption peak of Ag NPs was examined using UV- 2450 (Shimadzu) from 300 to 600 nm. By this measurement, reduction of AgNO₃ to Ag⁺ ions was monitored. Morphological analysis of nanoparticles was carried out by Hitachi S-4500 FESEM analyzer. A drop of the sample was coated on to carbon film and dried for the analysis. Energy-dispersive X-ray spectroscopy (EDAX) was used to examine the metals and materials present in the synthesized material using Hitachi S-4500 instrument equipped with a Thermo EDAX attachments. High Resolution Transmission Electron Microscopy (HRTEM) analysis was done in



Fig. 1. Biosynthesis of Ag NPs.

order to determine the process of formation of Ag NPs and to study their size and shape. The analysis was performed by Jeol/JEM 2100, operating at 200 Kv. Samples for HRTEM grid was arranged through coating a drop of Ag NPs solution on carbon-coated copper grids. Dynamic Light Scattering is a method is performed to measure the particle size distributions in the range of 2–500 nm using the instrument Nanophox, Germany. It measures the particle size using the scattered light, which is passed from a laser source and it depends on the Rayleigh scattering from the suspended NPs.

The human lung cancer (A549) cell line was achieved from the National Centre for Cell Science (NCCS), Pune and facilitated to grow in Eagles Minimum Essential Medium (EMEM) and 10% Fetal Bovine Serum (FBS). The obtained cells were sustained at 37 °C, 100% relative humidity, 5% CO₂ and 95% air. By the inverted microscope, cell culture was continuously viewed to determine the absence of bacterial and fungal contaminants as well as quantity of confluence.

2.4. In- vitro cytotoxic activity

The cell viability test was made with the 3-(4, 5-dimethylthiazol-2-yl) –2, 5-diphenyltetrazolium bromide (MTT) assay to demonstrate the cytotoxic effect of Ag NPs and garlic extract. MTT is a tetrazolium salt which was used to investigate mitochondrial function. The enzymatic reduction of MTT was catalyzed by the mitochondrial succinate dehydrogenase enzyme, which breaks the tetrazolium ring, transforming it to a purple formazan which is not soluble (Mosmann, 1983). Consequently, the quantity of formazan formed is proportionate to the quantity of viable cells. A549 cells were taken in a 96-well plate at the density of 5×10^3 cells/well. The cells were grown in a 96-well plate for 24 hrs, in 200 μ l of EMEM with 10% FBS. After 24 hrs, cells were

exposed to Ag NPs at a different dose (1–20 mg/ml) for a period of 48 hrs. Each well in the plate containing the cells were then subjected to 15 μ l of MTT (5 mg/ml) and incubated for 4 hrs at 37 °C. EMEM was then removed, and 100 μ l of DMSO was added to each well and then measured using the microplate reader at 570 nm. EMEM without samples was served as control.

$$\% \text{ Cell viability} = 100 - \text{Abs}(\text{sample}) / \text{Abs}(\text{control}) \times 100$$

3. Results and discussion

3.1. PXRD analysis

Fig. 2a shows the PXRD pattern of Ag NPs synthesized from ethanol extract of garlic powder. From the Figure, the primary diffraction peaks at 2θ values of 28.05°, 32.41°, 38.31°, 46.38°, 55.01°, 57.62°, 67.68° and 77.61° respectively for (100), (110), (111), (200), (211), (211), (220) and (311) planes belonging to AgNP, which are well matched with standard JCPDS: 76–1393. The average size of the Ag NPs was determined from the PXRD pattern, according to the peak and line width of the plane, using Scherer's equation (Parikh et al., 2011).

$$D = K\lambda / \beta \cos(\theta)$$

Where, 'D' denotes diameter, 'K' represents the shape factor (0.94), ' λ ' denotes the wavelength of the X-ray, ' β ' represents angular width at FWHM of the X-ray diffraction peak at Bragg's diffraction angle ' θ '. The results revealed that the average size of the Ag NPs was found to be 12 nm. Table 1 shows the PXRD parameters along with the particle size of each 2θ values. The Table revealed that, the obtained particle size in the present work is better than Ag NPs synthesized from aqueous Garlic extract (Theivasanthi

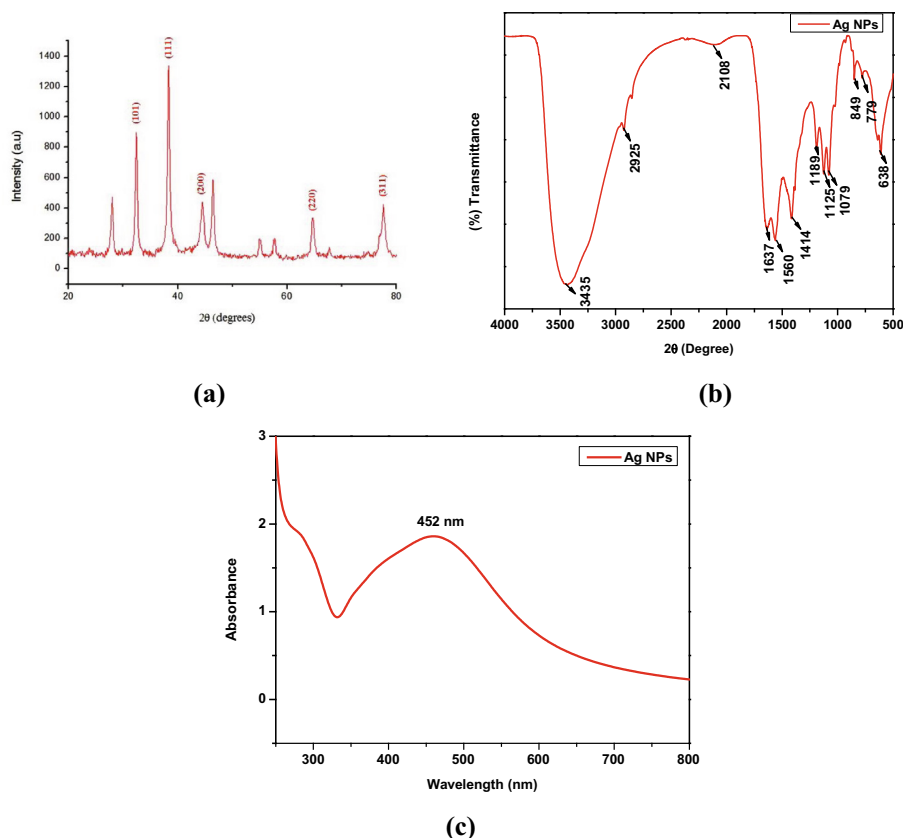


Fig. 2. (a) XRD pattern, (b) FTIR spectrum and (c)Uv-Visible spectrum of AgNPs.

Table 1Powdered XRD data and particle size of AgNPs synthesized using *A. sativum* extract.

Pos. [$^{\circ}$ 2Th.]	Height [cts]	FWHM Left [$^{\circ}$ 2Th.]	d-spacing [Å]	Rel. Int. [%]	Particle size in nm
32.1484	16.74	0.5904	2.78435	22.67	14.63
38.1740	73.87	0.5904	2.35758	100.00	14.87
44.2981	13.41	1.5744	2.04483	18.16	15.60
64.3723	23.48	0.7872	1.44730	31.79	12.46
77.6489	21.55	0.9840	1.22969	29.18	10.83
Average size of the nanoparticles 11.7					

and Alagar, 2012). The defects that occurred in the nanoparticles was calculated by the dislocation density (δ), as follows (Logeswari et al., 2015).

$$\delta = 1/D^2$$

Where D = crystallite size.

The dislocation density (δ) of Ag NPs was calculated as $6.94 \times 10^{-3} \text{ (nm)}^{-2}$. Table 2 shows the comparative dislocation density (δ) of Ag NPs prepared from aqueous Garlic extract. From the Table, the dislocation density of Ag NPs synthesized from *Allium sativum* has lesser defects owing to its better Surface Plasmon Resonance (SPR) properties and larger surface area compared to previous reports.

3.2. FT-IR spectroscopy

The FT-IR spectrum for Ag NPs synthesized using garlic extract, showed a variation in the intensity of bands in different regions (Fig. 2b). The peak at 3434 cm^{-1} was assigned to the -O-H stretching vibrations indicating the presence of hydroxyl groups. The peaks at 2925 cm^{-1} and 2108 cm^{-1} were due to the strong intensity of alkyl (-CH₂-) group. The peak at 1637 cm^{-1} and 1560 cm^{-1} was assigned to aryl aromatic ring. The O-H band corresponds to the peak at 1414 cm^{-1} . The peaks arise at 1385 , 1189 , 1125 and 1079 cm^{-1} indicate the C-N stretch, which contributes to the presence of amine group in the synthesized material. The presence of sulfur compounds was primarily confirmed by the bands formed at 849 , 779 and 638 cm^{-1} . The analysis confirmed the available functional groups may act as reducing and stabilizing agents for Ag NPs, either by carbonyl groups or sulfur containing groups (Saha et al., 2017).

3.3. UV-Vis spectral analysis

UV-Visible absorption spectroscopy is an important tool to identifying the formation and stability of metal NPs in an aqueous solution. The extracellular synthesis of Ag NPs using *A. sativum* extract involved in the reduction was identified by the UV-Visible spectroscopy and shown in Fig. 2c. The dark brown colour was observed from the synthesized Ag NPs which indicates the reduction of pure Ag⁺ ions due to its SPR properties (Varshney et al., 2009). The surface plasmon absorption band is observed at 452 nm in UV-Visible spectrum for *A. sativum* extract due to electronic transitions from the valence band to the conduction band, which indicates the formation of Ag NPs (Paul et al., 2015).

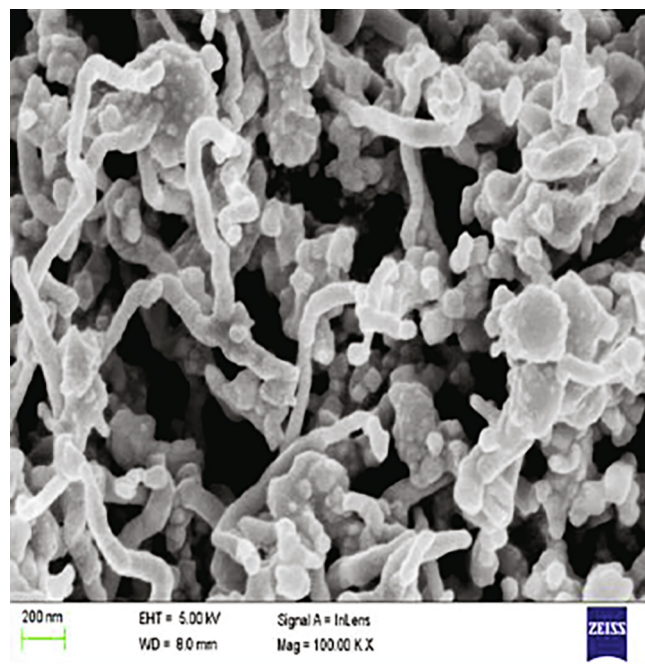
Table 2

Comparison of dislocation density of Ag NPs synthesized from various extracts.

Material	Dislocation density (δ)	Ref
Ag NPs (<i>Eucalyptus gloopus</i>)	$7.18 \times 10^{-3} \text{ (nm)}^{-2}$	
Ag NPs (<i>Azadirachta indica</i>)	$9.07 \times 10^{-3} \text{ (nm)}^{-2}$	Senthilkumar et al., 2018a;
Ag NPs (<i>Coriandrum sativum</i>)	$7.30 \times 10^{-3} \text{ (nm)}^{-2}$	Senthilkumar et al., 2018b
Ag NPs (<i>Allium sativum</i>)	$6.94 \times 10^{-3} \text{ (nm)}^{-2}$	[Present work]

3.4. FESEM and EDAX

Fig. 3 depicts the typical FESEM image of green synthesized Ag NPs. The image depicts that the particles are spherical and rod shaped with an average size around 70 nm. EDAX spectrum of Ag NPs synthesized from ethanol extract of garlic is presented in Fig. 4. Figure shows the signal at 3 keV in the EDAX spectrum revealed that the existence of silver, which is a unique feature for the absorption of metallic silver nanocrystallites owing to their SPR property (Mahendran and RanjithaKumari, 2016). Also, the spectrum exhibits Ag, C and O elements only and no other impurities were present in the prepared Ag NPs. Also, Figure shows the weight percentage of elemental constituents such as silver 58.34%, carbon 12.79% and oxygen 28.87%. According to the findings of Otunola et al., 2017 the weight percentage of Ag NPs synthesized from aqueous extract of garlic was 57.16% which showed that better yield was obtained in the present investigation.

**Fig. 3.** FESEM of Ag NPs.

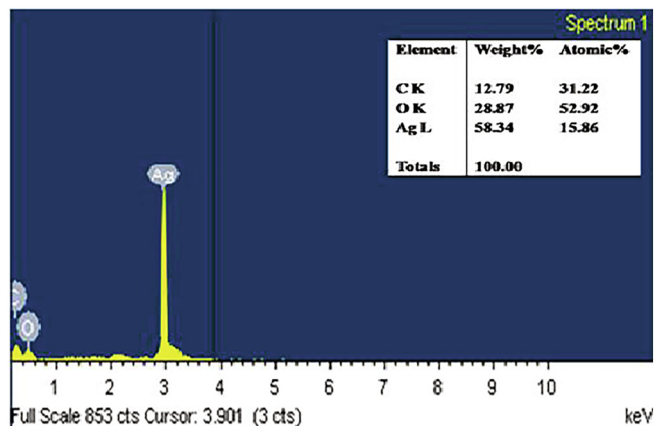


Fig. 4. EDAX spectrum of Ag NPs.

3.5. HRTEM analysis

A typical HRTEM image of biologically synthesized Ag NPs suggests that the particles were well segregated and distributed without any agglomeration. The stabilization of the category of Ag NPs is due to the domination of carbonyl and hydroxyl groups which give weak electrostatic interactions between Ag NPs and functional groups from garlic extract. Also, most of the particles were spherical shaped with varying size of 10–40 nm which is shown in Fig. 5a. The crystalline nature of the synthesized NPs was characterized by Selected Area Electron Diffraction (SAED) pattern and shown in Fig. 5b. The SAED pattern clearly shows the characteristic polycrystalline ring pattern for a FCC structure which exactly coincide with results of PXRD pattern (Mehmood et al., 2014). The sizes

of the Ag NPs have been determined and the distribution of Ag NPs is shown in Fig. 5c. It indicated that the distribution with an average mean size of 30 nm. Green synthesized biocompatible nanoparticles synthesized using citrate and stabilized with garlic extract showed increase in size and polydispersity in TEM analysis (White et al., 2012). In another study, TEM micrograph of Ag NPs synthesized using *A. sativum* extract showed quasi spherical particles with an average size of 170 nm (Mohamed et al., 2022).

3.6. Dynamic light scattering (DLS)

Fig. 6 shows the DLS analysis which depict the Ag NPs particle size. From the analysis, the mean particle size of Ag NPs was observed between 3 nm and 10 nm. The comparison table of previously reported distribution of Ag NPs based on size is shown in Table 3. From the Table, the size of the synthesized NPs are very

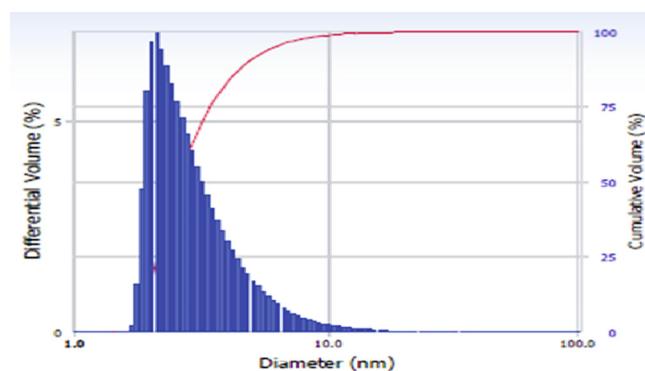


Fig. 6. DLS spectrum of Ag NPs.

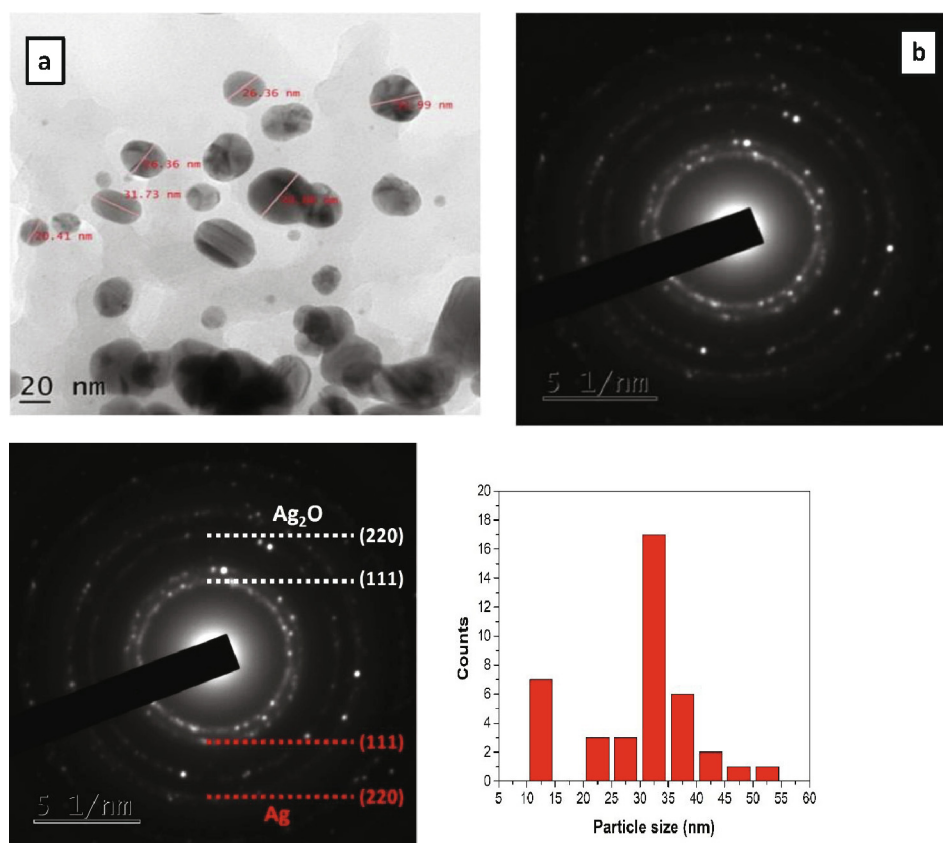


Fig. 5. (a) HRTEM and (b) SAED pattern of Ag NPs.

Table 3
Comparison of particle size distribution of Ag NPs synthesized from various extracts.

Sl.No	Material	Particle Size	Extract	Reference
1	Ag NPs	37.44, 40.06, 46.65 and 53.37 nm	<i>Coriandrum sativum</i> leaf, stem, seed and root	Senthilkumar et al., 2018a
2	Ag NPs	44, 53 and 85 nm	<i>Eucalyptus glopus</i> , <i>Azadirachta indica</i> and <i>Coriandrum sativum</i> leaves	Senthilkumar et al., 2018b
3	Ag NPs	3–10 nm	<i>Allium sativum</i>	[Present work]

less when compared to previously reported size values, which confirms the prepared Ag NPs from garlic extract has hydrodynamic size and polydispersity in nature.

3.7. In-vitro cytotoxicity

Assessment of cytotoxicity plays a major role for evaluation in toxicology when assessing its effectiveness as a drug that elucidate the cellular response to a toxicant. In the present study, the cytotoxicity impact on cell inhibition was examined by a dose-dependent approach at different concentration. Figs. 7a and 7b respectively shows the efficiency of synthesized Ag NPs and *A. sativum* extract alone in inhibiting cancer cells. From the Figures, it is evident that the percentage of cell viability was reduced by increasing concentration of Ag NPs and extract. Also, it is confirmed that, the required concentration of Ag NPs required was

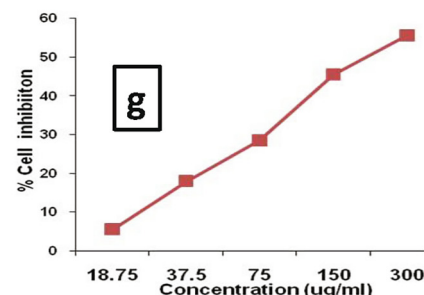
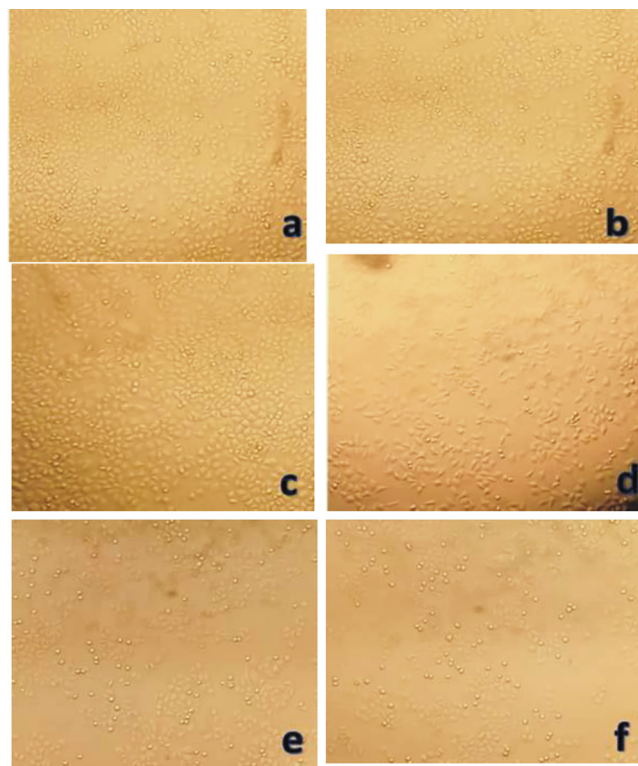


Fig. 7b. In-vitro cytotoxic activity of the ethanol garlic extract against A549 cell line. (a) Untreated A549 cell line (b) 18.75 µg/ml (c) 37.5 µg/ml (d) 75 µg/ml (e) 150 µg/ml (f) 300 µg/ml (g) Percentage of cell inhibition of *A. sativum* extract against A549 cell line.

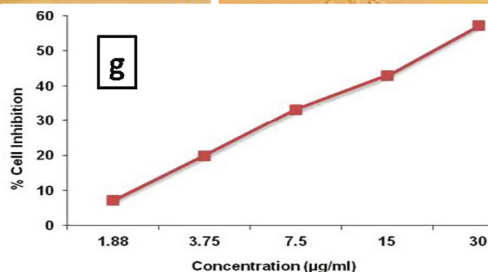
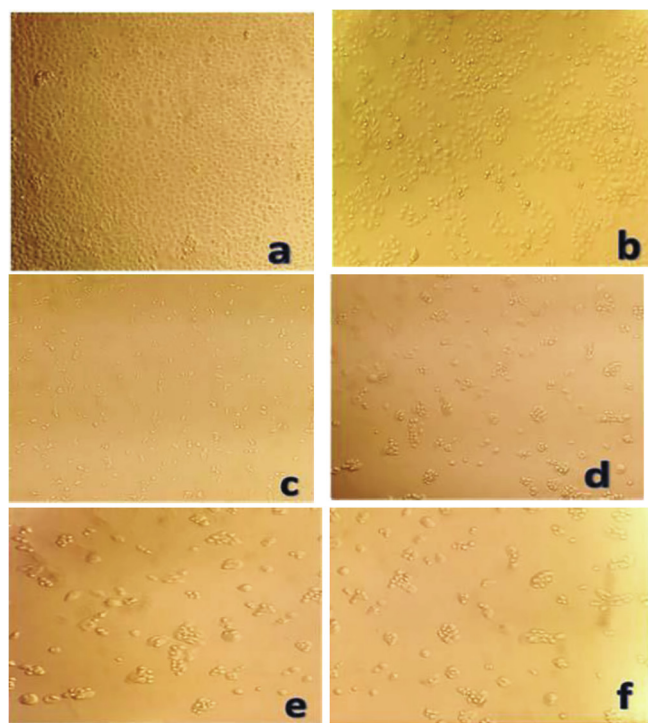


Fig. 7a. In-vitro cytotoxic activity of the biosynthesized Ag NPs against A549 cell line. (a) Untreated A549 cell line, (b) Ag NPs – 1.88 µg/ml, (c) Ag NPs – 3.75 µg/ml, (d) AgNPs – 7.5 µg/ml (e) Ag NPs – 15 µg/ml, (f) Ag NPs – 30 µg/ml (g) Percentage of cell inhibition of Ag NPs against A549 cell line.

minimum when compared to the concentration of the extract (*A. Sativum*). This increasing cell inhibition activity with a higher concentration of Ag NPs indicated that more number of Ag NPs can penetrate into the cancer cells and finally leading to cell death. For the comparison, a plot has been drawn between concentration and the percentage of cell inhibition and shown in Figure 9a (g) and Figure 9b (g). From the Figures, it is observed that, 50% of cell inhibition was observed by adding 22 µg/ml of Ag NPs fabricated from ethanol extract of *A. sativum*. At the same time, the same cell inhibition was achieved by adding 177 µg/ml of pure *A. Sativum* extract, which shows the better cytotoxicity effect attained from

the biologically synthesized Ag NPs due to ROS prompting and leads to cellular impairment and cell death (Jacob et al., 2012; Sankar et al., 2013). The cytotoxic effects of Ag NPs are higher in cancer cells when compared to normal cells. The small size and the large surface to volume ratio help in penetrating the cells easily. The major mechanism of cancer cell inhibition by metallic nanoparticles includes Reactive oxygen species generation, Caspase-3 activation, modification of mitochondrial membrane potential and DNA damage (Andleeb et al., 2021). Hence, from the observations, it was confirmed that the material proposed in the present work shows good inhibition activity against A549 cancer cell line.

4. Conclusion

An efficient biomediated Ag NPs was synthesized from an ethanol extract of *A.sativum* for the first time. The observed changes in the colour and the peak observed due to SPR at 345 nm in UV-Vis-NIR spectrum confirms the formation of material. The morphology of the material was also correlated from FESEM and HRTEM images. FTIR analysis shows the possible functional groups present in the synthesized material. The results revealed that Ag NPs were crystalline in nature and were spherical shaped with an average size of 30 nm. The efficiency of cytotoxicity effect has been showed the promising cytotoxicity activity against A549 cell line from synthesized Ag NPs using *A. sativum* extract when compare to pure extract. It is concluded that the prepared Ag NPs via *A.sativum* has good efficiency to possess high cytotoxicity due to induce reactive oxygen species and cause cellular damage leading to cell death, which suggests the potential therapeutic use of Ag NPs synthesized from ethanol extract of *A.sativum*.

Declaration of Competing Interest

The authors declare that they have no known competing financial interests or personal relationships that could have appeared to influence the work reported in this paper.

Acknowledgement

The authors extend thrie appreciation to the Researchers supporting project number (RSP-2022R479) King Saud University, Riyadh, Saudi Arabia and DST-SERB -Project Ref. No. SB/EMEQ-431/2014, Department of Science and Technology, New Delhi, India.

References

Andleeb, A., Andleeb, A., Asghar, S., Zaman, G., Tariq, M., Mehmood, A., Nadeem, M., Hano, C., Lorenzo, J.M., Abbasi, B.H., 2021. A Systematic Review of Biosynthesized Metallic Nanoparticles as a Promising Anti-Cancer-Strategy. *Cancers. Basel*, 13, 2818.

Bouqellah, N.A., Mohamed, M.M., Ibrahim, Y., 2019. Synthesis of eco-friendly silver nanoparticles using *Allium sp.* and their antimicrobial potential on selected vaginal bacteria. *Saudi J Biol Sci.* 26, 1789–1794.

Burda, C., Chen, X., Narayanan, R., El-sayed, M.A., 2005. Chemistry and properties of nanocrystals of different shapes. *Chemical Reviews* 105, 1025–1102.

Castro-Aceituno, V.K., Ahn, S., Simu, S.Y., Priyanka, S., Ramya, M., Hyun, A., Lee Yang, D.C., 2016. Anticancer activity of silver nanoparticles from *Panax ginseng* fresh leaves in human cancer cells. *Biomed. Pharmacother.* 84, 158–165.

El-Refai, A.A., Ghoniem, A.G., El-Khateeb, A.Y., Hassaan, M.M., 2018. Eco-friendly synthesis of metal nanoparticles using ginger and garlic extracts as biocompatible novel antioxidant and antimicrobial agents. *J. Nanostructure Chem.* 8, 71–81.

Ezhilarasi, A.A., Vijaya, J.J., Kaviyarasu, K., Kennedy, J.L., Ramalingam, R.J., Al-Lohedan, H.A., 2018. Green synthesis of NiO nanoparticles using Aegle marmelos leaf extract for the evaluation of in-vitro cytotoxicity, antibacterial and photocatalytic properties. *J Photochem Photobiol B.* 180, 39–50.

Fall, A., Ngom, I., Bakayoko, S., M., Mohamed, N.,, Jadvi, H.,, Kaviyarasu, K., Ngom, K., Diop, B., 2020. Biosynthesis of TiO2 nanoparticles by using natural extract of *Citrus sinensis*. *Materials Today: Proceedings.* 36.

Fleischauer, A.T., Arab, L., 2001. Garlic and Cancer: A Critical Review of the Epidemiologic Literature. *J. of Nutr.* 131, 1032–1040.

He, Y., Du, Z., Ma, S., Liu, Y., Li, D., Huang, H., Jiang, S., Cheng, S., Wu, W., Zhang, K., Zheng, X., 2016. Effects of green-synthesized silver nanoparticles on lung cancer cells *in-vitro* and grown as xenograft tumors *in vivo*. *Int. J. Nanomed.* 11, 1879–1887.

Jacob, S.J.P., Finub, J.S., Narayanan, A., 2012. Synthesis of silver nanoparticles using *Piper longum* leaf extracts and its cytotoxic activity against Hep-2 cell line. *Coll. and Surf. B.* 91, 212–214.

Jayapriya, M., Dhanasekaran, D., Arulmozhi, M., Nandhakuma, r, E., Senthilkumar, N., Sureshkumar, K., 2019. Green synthesis of silver nanoparticles using *Piper longum* catk in extract irradiated by sunlight: antibacterial and catalytic activity. *Res. Chem. Intermediates.* 45, 3617–3631.

Jeyabharathi, S., Naveenkumar, S., Chandramohan, S., Venkateshan, N., Gawwad, A., Mohamed, S.E., Rasheed, R.A., Farraj, D.A.A., Muthukumar, A., 2022. Biological synthesis of zinc oxide nanoparticles from the plant extract, *Wattakaka volubilis* showed anti-microbial and anti-hyperglycemic effects. *J. King Saud Univ. Sci.* 34, 101881.

Jin, Z.Y., Wu, M., Han, R.Q., Zhang, X.F., Wang, X.S., Liu, A.M., Zhou, J.Y., Lu, Q.Y., Zhang, Z.F., Zhao, J.K., 2013. Raw garlic consumption as a protective factor for lung cancer, a population-based case-control study in a Chinese population. *Cun. Prevent. Res.* 6, 711–718.

Lin, J., Opak, A.R., Keller, M.G., Hutchings, A.D., Terblanch, e, S., E., Jager, A. K., Van, Staden, J., 1999. Preliminary screening of some traditional zulu medicinal plants for anti-inflammatory and antimicrobial activities. *J. Ethnopharmacol.* 68, 267–274.

Logeswari, P., Silambarasan, S., Jayanthi, A., 2015. Synthesis of silver nanoparticles using plants extract and analysis of their antimicrobial property. *J. Saudi Chem. Soc.* 19, 311–317.

Mahendran, G., RanjithaKumari, B.D., 2016. Biological activities of silver nanoparticles from *Nothapodytesnimmoniana* (Graham) Mabb. *Fruit extracts. Food Sci. and Human Wellness.* 5, 207–218.

Mehmood, A., Murtaza, G., Bhatti, T.M., Raffi, M., Kausar, R., 2014. Antibacterial efficacy of silver nanoparticles synthesized by a green method using bark extract of *Meliaazedarach*. *L. The J. of Pharma. Innov.* 9, 238–245.

Mohamed, J.M.M., Alqahtani, A., Kumar, T.V.A., Fateah, A.A., Alqahtani, T., Krishnaraju, V., Ahmad, F., Mena, F., Alamri, A., Muthumani, R., Vijaya, R., 2022. Superfast Synthesis of Stabilized Silver Nanoparticles Using Aqueous *Allium sativum* (Garlic) Extract and Isoniazid Hydrazide Conjugates: Molecular Docking and In-Vitro Characterizations. *Molecules.* 27, 110.

Mosmann, T., 1983. Rapid colorimetric assay for cellular growth and survival: Application to proliferation and cytotoxicity assays. *J. Immunol. Methods.* 65, 55–63.

Murugesan, S., Bhuvanewari, S., Sivamurugan, V., 2017. Green Synthesis, characterization of Silver Nanoparticles of A Marine Red *Alga Spyridia Fusiformis* and their Antibacterial Activity. *Int. J. Pharmacy. and Pharmac Sci.* 9, 192–197.

Ocoy, I., Demirbas, A., McLamore, E.S., Altinsoy, B., Ildiz, N., Baldemir, A., 2017. Green synthesis with incorporated hydrothermal approaches for silver nanoparticles formation and enhanced antimicrobial activity against bacterial and fungal pathogens. *J. Mol. Liq.* 238, 263–269.

Onitsuka, S., Hamada, T., Okamura, H., 2019. Preparation of antimicrobial gold and silver nanoparticles from tea leaf extracts. *Coll. and Surf.B.* 173, 242–248.

Otunola, G.A., Afolayan, A.J., Ajayi, E.O., Odeyemi, S.W., 2017. Characterization, Antibacterial and Antioxidant Properties of Silver Nanoparticles Synthesized from Aqueous Extracts of *Allium sativum*, *Zingiberofficinale*, and *Capsicum frutescens*. *Pharmacogn. Mag.* 13, S201–S208.

Parikh, R.Y., Ramanathan, R., Coloe, P.J., Bhargava, S.K., Patole, M.S., Shouche, Y.S., Bansal, V., 2011. Genus-wide physicochemical evidence of extracellular crystalline silver nanoparticles biosynthesis by *Morganella* spp. *PLoS One.* 6, 1–7.

Pattanayak, S., Mollick, M.R., Maity, D., Sharmila, C., Kumar Dash, S., Sourav, C., Roy, S., Chattopadhyay, D., Chakraborty, M., 2017. Buteamonosperma bark extract mediated green synthesis of silver nanoparticles: Characterization and biomedical applications. *J. Saudi Chem. Soc.* 21, 673–684.

Paul, J.A., KarunaiSelvi, B., Karmegam, N., 2015. Biosynthesis of silver nanoparticles from *Premnaserratifolia* L.leaf and its anticancer activity in CCl4-induced hepato-cancerous Swiss albino mice. *Appl. Nanosci.* 5, 937–944.

Philipa, D., Unni, C., Aromal, A.S., Vidhu, V.K., 2011. *Murraya Koenigii* leaf-assisted rapid green synthesis of silver and gold nanoparticles. *SpectroActa Part A* 78, 899–904.

Rahman, K., Billington, D., 2000. Dietary supplementation with aged garlic extract inhibits ADP-induced platelet aggregation in humans. *The J. of Nutr.* 130, 2662–2665.

Saha, M., Bandyopadhyay, P.K., 2017. Green Biosynthesis of Silver Nanoparticle Using Garlic, *Allium sativum* with Reference to Its Antimicrobial Activity against the Pathogenic Strain of *Bacillus sp.* and *Pseudomonas sp.* Infecting Goldfish, *Carassiusauratus*, *Proceedings of the Zoological Society.* DOI: <https://doi.org/10.1007/s12595-017-0258-3>.

Sankar, R., Karthik, A., Prabu, A., Karthik, S., Subramanian, K., Shivashangari Ravikumar, V., 2013. *Origanum vulgare* mediated biosynthesis of silver nanoparticles for its antibacterial and anticancer activity. *Coll. and Surf.B.* 108, 80–84.

Selvan, A.D., Mahendiran, D., Senthil Kumar, R., Kalilurrahman, A., 2018. Garlic, green tea and turmeric extracts-mediated green synthesis of silver

- nanoparticles: Phytochemical, antioxidant and *in-vitro* cytotoxicity studies. *J. Photochem. and Photobiol. B.* 180, 243–252.
- Selvan, S.T., Tan, T.T.Y., Yi, D.K., Jana, J.R., 2010. Functional and multifunctional nanoparticles for bioimaging and biosensing. *Langmuir* 26, 11631–11641.
- Senthilkumar, N., Aravindhan, V., Ruckmani, K., VethaPothheher, I., 2018a. *Coriandrum sativum* Mediated Synthesis of Silver Nanoparticles and Evaluation of their Biological Characteristics. *Mater. Res. Express.* 5, 1–23.
- Senthilkumar, N., Arulraj, A., Nandhakumar, E., Ganapathy, M., Vimalan, M., VethaPothheher, I., 2018b. Green mediated synthesis of plasmonic nanoparticle (Ag) for antireflection coating in bare mono silicon solar cell. *Material Sci: Mat. Electro.* 29, 12744–12753.
- Sevilla, P., 2013. Molecular characterization of drug's nanocarriers based on plasmon-enhanced spectroscopy: fluorescence (SEF) and Raman (SERS). *Optica Pura Y Aplicada* 46, 111–119.
- Shume, W.M., Murthy, H.C.A., Zereffa, E.A., 2020. A Review on Synthesis and Characterization of Ag₂O Nanoparticles for Photocatalytic Applications. *J. Chem.* 2020, 1–15.
- Susheela, S., Sunil, B.D., Kumar, Bulchandani, S., T., Shelza, B., 2013. Green Synthesis of Silver Nanoparticles and their Antimicrobial Activity against Gram Positive and Gram Negative Bacteria. *Int. J. Biotech.andBioeng.Res.* 4, 711–714.
- Theivasanthi, T., Alagar, M., 2012. Electrolytic synthesis and characterizations of silver nanopowder. *NanoBiomed.andEngin.* 4, 58–65.
- Thomas, B., Vithiya, B.S.M., Prasad, T.A.A., Mohamed, S.B., Magdalane, C.M., Kaviyarasu, K., Maaza, M., 2019. Antioxidant and Photocatalytic Activity of Aqueous Leaf Extract Mediated Green Synthesis of Silver Nanoparticles Using *Passiflora edulis f. flavicarpa*. *J. Nanosci Nanotechnol.* 19, 2640–2648.
- Valsalam, S., Agastian, P., Arasu, M.V., Al-Dhabi, N.A., Ghilan, A.M., Kaviyarasu, K., Ravindran, B., Chang, S.W., Arokiyaraj, S., 2019. Rapid biosynthesis and characterization of silver nanoparticles from the leaf extract of *Tropaeolum majus* L. and its enhanced *in-vitro* antibacterial, antifungal, antioxidant and anticancer properties. *J. Photochem Photobiol B.* 191, 65–74.
- Varshney, R., Mishra, A.N., Bhadauria, S., Gaura, M.S., 2009. A Novel microbial route to synthesize silver nanoparticles using fungus *Hormoconisresinae*. *Digest J of Nanomat. And Biostruct.* 4, 349–355.
- White, G., Kerscher, P., Brown, R.M., Morella, J.D., McAllister, W., Dean, D., Kitchens, C.L., 2012. Green Synthesis of Robust, Biocompatible Silver Nanoparticles Using Garlic Extract. *J. Nanomater.* 2012, 730746.
- Zappa, C., Mousa, S.A., 2016. Non-small cell lung cancer: current treatment and future advances. *Transl Lung Cancer Res.* 5, 288–300.